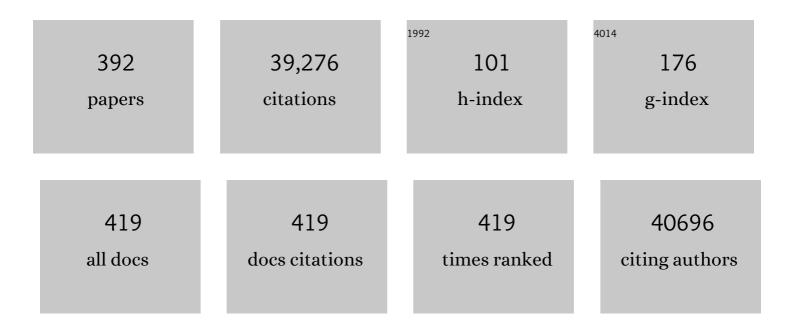
David Ian Stuart

List of Publications by Year in descending order

Source: https://exaly.com/author-pdf/4036243/publications.pdf Version: 2024-02-01



ΠΑΝΙ Ο ΤΗΛΡΤ

#	Article	IF	CITATIONS
1	Broad and strong memory CD4+ and CD8+ T cells induced by SARS-CoV-2 in UK convalescent individuals following COVID-19. Nature Immunology, 2020, 21, 1336-1345.	14.5	1,066
2	Evidence of escape of SARS-CoV-2 variant B.1.351 from natural and vaccine-induced sera. Cell, 2021, 184, 2348-2361.e6.	28.9	936
3	The three-dimensional structure of foot-and-mouth disease virus at 2.9 Ã resolution. Nature, 1989, 337, 709-716.	27.8	887
4	Antibody Status and Incidence of SARS-CoV-2 Infection in Health Care Workers. New England Journal of Medicine, 2021, 384, 533-540.	27.0	803
5	SARS-CoV-2 Omicron-B.1.1.529 leads to widespread escape from neutralizing antibody responses. Cell, 2022, 185, 467-484.e15.	28.9	788
6	Protein production and purification. Nature Methods, 2008, 5, 135-146.	19.0	763
7	Structural basis for the recognition of hydroxyproline in HIF-11 [±] by pVHL. Nature, 2002, 417, 975-978.	27.8	651
8	Reduced neutralization of SARS-CoV-2 B.1.617 by vaccine and convalescent serum. Cell, 2021, 184, 4220-4236.e13.	28.9	630
9	The Interaction Properties of Costimulatory Molecules Revisited. Immunity, 2002, 17, 201-210.	14.3	587
10	The atomic structure of the bluetongue virus core. Nature, 1998, 395, 470-478.	27.8	543
11	Antibody escape of SARS-CoV-2 Omicron BA.4 and BA.5 from vaccine and BA.1 serum. Cell, 2022, 185, 2422-2433.e13.	28.9	532
12	Antibody evasion by the P.1 strain of SARS-CoV-2. Cell, 2021, 184, 2939-2954.e9.	28.9	519
13	High resolution structures of HIV-1 RT from four RT–inhibitor complexes. Nature Structural and Molecular Biology, 1995, 2, 293-302.	8.2	514
14	A functional and structural basis for TCR cross-reactivity in multiple sclerosis. Nature Immunology, 2002, 3, 940-943.	14.5	500
15	A versatile ligation-independent cloning method suitable for high-throughput expression screening applications. Nucleic Acids Research, 2007, 35, e45-e45.	14.5	499
16	Lysine Methylation as a Routine Rescue Strategy for Protein Crystallization. Structure, 2006, 14, 1617-1622.	3.3	483
17	Crystal structure of cat muscle pyruvate kinase at a resolution of 2.6 Ã Journal of Molecular Biology, 1979, 134, 109-142.	4.2	459
18	A mechanism for initiating RNA-dependent RNA polymerization. Nature, 2001, 410, 235-240.	27.8	458

#	Article	IF	CITATIONS
19	Reduced neutralization of SARS-CoV-2 B.1.1.7 variant by convalescent and vaccine sera. Cell, 2021, 184, 2201-2211.e7.	28.9	442
20	Neutralizing nanobodies bind SARS-CoV-2 spike RBD and block interaction with ACE2. Nature Structural and Molecular Biology, 2020, 27, 846-854.	8.2	434
21	Crystal structure of the complex between human CD8 $\hat{l}\pm\hat{l}\pm$ and HLA-A2. Nature, 1997, 387, 630-634.	27.8	428
22	Mechanism of inhibition of HIV-1 reverse transcriptase by non-nucleoside inhibitors. Nature Structural and Molecular Biology, 1995, 2, 303-308.	8.2	415
23	Fitness Cost of Escape Mutations in p24 Gag in Association with Control of Human Immunodeficiency Virus Type 1. Journal of Virology, 2006, 80, 3617-3623.	3.4	408
24	Structure of a major immunogenic site on foot-and-mouth disease virus. Nature, 1993, 362, 566-568.	27.8	360
25	Complexes of HIV-1 Reverse Transcriptase with Inhibitors of the HEPT Series Reveal Conformational Changes Relevant to the Design of Potent Non-Nucleoside Inhibitors. Journal of Medicinal Chemistry, 1996, 39, 1589-1600.	6.4	353
26	What does structure tell us about virus evolution?. Current Opinion in Structural Biology, 2005, 15, 655-663.	5.7	348
27	A sensor-adaptor mechanism for enterovirus uncoating from structures of EV71. Nature Structural and Molecular Biology, 2012, 19, 424-429.	8.2	347
28	Performance characteristics of five immunoassays for SARS-CoV-2: a head-to-head benchmark comparison. Lancet Infectious Diseases, The, 2020, 20, 1390-1400.	9.1	336
29	The antigenic anatomy of SARS-CoV-2 receptor binding domain. Cell, 2021, 184, 2183-2200.e22.	28.9	331
30	Crystal structure at 2.8 Ã resolution of a soluble form of the cell adhesion molecule CD2. Nature, 1992, 360, 232-239.	27.8	330
31	Neutralization of SARS-CoV-2 by Destruction of the Prefusion Spike. Cell Host and Microbe, 2020, 28, 445-454.e6.	11.0	298
32	A structural basis for immunodominant human T cell receptor recognition. Nature Immunology, 2003, 4, 657-663.	14.5	290
33	Structure and functionality in flavivirus NS-proteins: Perspectives for drug design. Antiviral Research, 2010, 87, 125-148.	4.1	289
34	The Crystal Structure of Plasma Gelsolin: Implications for Actin Severing, Capping, and Nucleation. Cell, 1997, 90, 661-670.	28.9	273
35	Glycoprotein Structural Genomics: Solving the Glycosylation Problem. Structure, 2007, 15, 267-273.	3.3	273
36	Structural basis for the neutralization of SARS-CoV-2 by an antibody from a convalescent patient. Nature Structural and Molecular Biology, 2020, 27, 950-958.	8.2	268

#	Article	IF	CITATIONS
37	A mechanical explanation of RNA pseudoknot function in programmed ribosomal frameshifting. Nature, 2006, 441, 244-247.	27.8	267
38	Antibody responses to SARS-CoV-2 vaccines in 45,965 adults from the general population of the United Kingdom. Nature Microbiology, 2021, 6, 1140-1149.	13.3	254
39	Structural Basis for the Resilience of Efavirenz (DMP-266) to Drug Resistance Mutations in HIV-1 Reverse Transcriptase. Structure, 2000, 8, 1089-1094.	3.3	253
40	Structure Unifies the Viral Universe. Annual Review of Biochemistry, 2012, 81, 795-822.	11.1	252
41	Insights into assembly from structural analysis of bacteriophage PRD1. Nature, 2004, 432, 68-74.	27.8	246
42	Structure of the TRAIL-DR5 complex reveals mechanisms conferring specificity in apoptotic initiation. Nature Structural Biology, 1999, 6, 1048-1053.	9.7	235
43	The Duration, Dynamics, and Determinants of Severe Acute Respiratory Syndrome Coronavirus 2 (SARS-CoV-2) Antibody Responses in Individual Healthcare Workers. Clinical Infectious Diseases, 2021, 73, e699-e709.	5.8	235
44	A procedure for setting up high-throughput nanolitre crystallization experiments. Crystallization workflow for initial screening, automated storage, imaging and optimization. Acta Crystallographica Section D: Biological Crystallography, 2005, 61, 651-657.	2.5	234
45	Towards rationalization of crystallization screening for small- to medium-sized academic laboratories: the PACT/JCSG+ strategy. Acta Crystallographica Section D: Biological Crystallography, 2005, 61, 1426-1431.	2.5	228
46	Structure and Dimerization of a Soluble Form of B7-1. Immunity, 2000, 12, 51-60.	14.3	227
47	Crystal structure of human α-lactalbumin at 1·7 à resolution. Journal of Molecular Biology, 1991, 221, 571-581.	4.2	225
48	The nsp9 Replicase Protein of SARS-Coronavirus, Structure and Functional Insights. Structure, 2004, 12, 341-353.	3.3	225
49	Localized reconstruction of subunits from electron cryomicroscopy images of macromolecular complexes. Nature Communications, 2015, 6, 8843.	12.8	225
50	Structural and serological evidence for a novel mechanism of antigenic variation in foot-and-mouth disease virus. Nature, 1990, 347, 569-572.	27.8	216
51	Toremifene interacts with and destabilizes the Ebola virus glycoprotein. Nature, 2016, 535, 169-172.	27.8	210
52	Crystal structure of SIV matrix antigen and implications for virus assembly. Nature, 1995, 378, 743-747.	27.8	202
53	The structure of HIV-1 reverse transcriptase complexed with 9-chloro-TIBO: lessons for inhibitor design. Structure, 1995, 3, 915-926.	3.3	201
54	Structural basis of Nipah and Hendra virus attachment to their cell-surface receptor ephrin-B2. Nature Structural and Molecular Biology, 2008, 15, 567-572.	8.2	200

#	Article	IF	CITATIONS
55	A COVID-19 vaccine candidate using SpyCatcher multimerization of the SARS-CoV-2 spike protein receptor-binding domain induces potent neutralising antibody responses. Nature Communications, 2021, 12, 542.	12.8	200
56	The postfusion structure of baculovirus gp64 supports a unified view of viral fusion machines. Nature Structural and Molecular Biology, 2008, 15, 1024-1030.	8.2	197
57	Differential occupational risks to healthcare workers from SARS-CoV-2 observed during a prospective observational study. ELife, 2020, 9, .	6.0	196
58	Structural Features Impose Tight Peptide Binding Specificity in the Nonclassical MHC Molecule HLA-E. Molecular Cell, 1998, 1, 531-541.	9.7	190
59	Structural basis of superantigen action inferred from crystal structure of toxic-shock syndrome toxin-1. Nature, 1994, 367, 94-97.	27.8	187
60	The Highly Ordered Double-Stranded RNA Genome of Bluetongue Virus Revealed by Crystallography. Cell, 1999, 97, 481-490.	28.9	181
61	Antibody testing for COVID-19: A report from theÂNational COVID Scientific Advisory Panel. Wellcome Open Research, 2020, 5, 139.	1.8	179
62	Paired Receptor Specificity Explained by Structures of Signal Regulatory Proteins Alone and Complexed with CD47. Molecular Cell, 2008, 31, 266-277.	9.7	171
63	An Altered Position of the $\hat{I}\pm2$ Helix of MHC Class I Is Revealed by the Crystal Structure of HLA-B*3501. Immunity, 1996, 4, 203-213.	14.3	169
64	The crystal structure of bluetongue virus VP7. Nature, 1995, 373, 167-170.	27.8	168
65	Hepatitis A virus and the origins of picornaviruses. Nature, 2015, 517, 85-88.	27.8	158
66	The crystal structure of the catalytic domain of human urokinase-type plasminogen activator. Structure, 1995, 3, 681-691.	3.3	155
67	Bound Water Structure and Polymorphic Amino Acids Act Together to Allow the Binding of Different Peptides to MHC Class I HLA-B53. Immunity, 1996, 4, 215-228.	14.3	155
68	Crystal structure of a soluble CD28-Fab complex. Nature Immunology, 2005, 6, 271-279.	14.5	153
69	Functional and structural studies of the vaccinia virus virulence factor N1 reveal a Bcl-2-like anti-apoptotic protein. Journal of General Virology, 2007, 88, 1656-1666.	2.9	153
70	Crystal structure of the extracellular region of the human cell adhesion molecule CD2 at 2.5Ã¥ resolution. Structure, 1994, 2, 755-766.	3.3	152
71	Atomic Snapshots of an RNA Packaging Motor Reveal Conformational Changes Linking ATP Hydrolysis to RNA Translocation. Cell, 2004, 118, 743-755.	28.9	151
72	Picornavirus uncoating intermediate captured in atomic detail. Nature Communications, 2013, 4, 1929.	12.8	148

#	Article	IF	CITATIONS
73	Evolution of Viral Structure. Theoretical Population Biology, 2002, 61, 461-470.	1.1	147
74	Antibody responses and correlates of protection in the general population after two doses of the ChAdOx1 or BNT162b2 vaccines. Nature Medicine, 2022, 28, 1072-1082.	30.7	147
75	Crystal structure of the RNA-dependent RNA polymerase from influenza C virus. Nature, 2015, 527, 114-117.	27.8	145
76	The ligand-binding face of the semaphorins revealed by the high-resolution crystal structure of SEMA4D. Nature Structural and Molecular Biology, 2003, 10, 843-848.	8.2	143
77	Antagonist HIV-1 Gag Peptides Induce Structural Changes in HLA B8. Journal of Experimental Medicine, 1996, 184, 2279-2286.	8.5	136
78	Vaccinia Virus Proteins A52 and B14 Share a Bcl-2–Like Fold but Have Evolved to Inhibit NF-κB rather than Apoptosis. PLoS Pathogens, 2008, 4, e1000128.	4.7	136
79	Membrane structure and interactions with protein and DNA in bacteriophage PRD1. Nature, 2004, 432, 122-125.	27.8	133
80	Lentiviral transduction of mammalian cells for fast, scalable and high-level production of soluble and membrane proteins. Nature Protocols, 2018, 13, 2991-3017.	12.0	131
81	Design of MKC-442 (Emivirine) Analogues with Improved Activity Against Drug-Resistant HIV Mutants. Journal of Medicinal Chemistry, 1999, 42, 4500-4505.	6.4	130
82	The structure of a cypovirus and the functional organization of dsRNA viruses. Nature Structural Biology, 1999, 6, 565-568.	9.7	129
83	The Human Low Affinity FcÎ ³ Receptors IIa, IIb, and III Bind IgG with Fast Kinetics and Distinct Thermodynamic Properties. Journal of Biological Chemistry, 2001, 276, 44898-44904.	3.4	127
84	Classical and Nonclassical Class I Major Histocompatibility Complex Molecules Exhibit Subtle Conformational Differences That Affect Binding to CD8αα. Journal of Biological Chemistry, 2000, 275, 15232-15238.	3.4	126
85	Rational Engineering of Recombinant Picornavirus Capsids to Produce Safe, Protective Vaccine Antigen. PLoS Pathogens, 2013, 9, e1003255.	4.7	126
86	Signaling Lymphocytic Activation Molecule (CDw150) Is Homophilic but Self-associates with Very Low Affinity. Journal of Biological Chemistry, 2000, 275, 28100-28109.	3.4	125
87	Implications of the HIV-1 Rev dimer structure at 3.2Ââ,,« resolution for multimeric binding to the Rev response element. Proceedings of the National Academy of Sciences of the United States of America, 2010, 107, 5810-5814.	7.1	124
88	Structure of a Pestivirus Envelope Glycoprotein E2 Clarifies Its Role in Cell Entry. Cell Reports, 2013, 3, 30-35.	6.4	124
89	Near-atomic structure of Japanese encephalitis virus reveals critical determinants of virulence and stability. Nature Communications, 2017, 8, 14.	12.8	117
90	Insights into Virus Evolution and Membrane Biogenesis from the Structure of the Marine Lipid-Containing Bacteriophage PM2. Molecular Cell, 2008, 31, 749-761.	9.7	116

#	Article	IF	CITATIONS
91	Crystal Structure of a Novel Conformational State of the Flavivirus NS3 Protein: Implications for Polyprotein Processing and Viral Replication. Journal of Virology, 2009, 83, 12895-12906.	3.4	115
92	Lessons from Structural Genomics. Annual Review of Biophysics, 2009, 38, 371-383.	10.0	115
93	An atomic model of the outer layer of the bluetongue virus core derived from X-ray crystallography and electron cryomicroscopy. Structure, 1997, 5, 885-893.	3.3	114
94	Structure of the Integrin Binding Fragment from Fibrillin-1 Gives New Insights into Microfibril Organization. Structure, 2004, 12, 717-729.	3.3	114
95	Structure of the Brain-Derived Neurotrophic Factor/Neurotrophin 3 Heterodimer. Biochemistry, 1995, 34, 4139-4146.	2.5	113
96	<i>In situ</i> macromolecular crystallography using microbeams. Acta Crystallographica Section D: Biological Crystallography, 2012, 68, 592-600.	2.5	113
97	Binding of the Second Generation Non-nucleoside Inhibitor S-1153 to HIV-1 Reverse Transcriptase Involves Extensive Main Chain Hydrogen Bonding. Journal of Biological Chemistry, 2000, 275, 14316-14320.	3.4	111
98	Killer Cell Immunoglobulin Receptors and T Cell Receptors Bind Peptide-Major Histocompatibility Complex Class I with Distinct Thermodynamic and Kinetic Properties. Journal of Biological Chemistry, 1999, 274, 28329-28334.	3.4	110
99	Crystal Structure and Carbohydrate Analysis of Nipah Virus Attachment Glycoprotein: a Template for Antiviral and Vaccine Design. Journal of Virology, 2008, 82, 11628-11636.	3.4	109
100	Evolution of Complex RNA Polymerases: The Complete Archaeal RNA Polymerase Structure. PLoS Biology, 2009, 7, e1000102.	5.6	109
101	Phenylethylthiazolylthiourea (PETT) Non-nucleoside Inhibitors of HIV-1 and HIV-2 Reverse Transcriptases. Journal of Biological Chemistry, 2000, 275, 5633-5639.	3.4	107
102	High-speed fixed-target serial virus crystallography. Nature Methods, 2017, 14, 805-810.	19.0	106
103	Evidence for the role of His-142 of protein 1C in the acid-induced disassembly of foot-and-mouth disease virus capsids. Journal of General Virology, 1999, 80, 1911-1918.	2.9	106
104	Tandem Fusion of Hepatitis B Core Antigen Allows Assembly of Virus-Like Particles in Bacteria and Plants with Enhanced Capacity to Accommodate Foreign Proteins. PLoS ONE, 2015, 10, e0120751.	2.5	105
105	Potent cross-reactive antibodies following Omicron breakthrough in vaccinees. Cell, 2022, 185, 2116-2131.e18.	28.9	105
106	Three-Dimensional Structures of Translating Ribosomes by Cryo-EM. Molecular Cell, 2004, 14, 57-66.	9.7	104
107	Specificity of the VP1 GH Loop of Foot-and-Mouth Disease Virus for $\hat{I}\pm\nu$ Integrins. Journal of Virology, 2006, 80, 9798-9810.	3.4	104
108	Structural and Functional Insights of RANKL–RANK Interaction and Signaling. Journal of Immunology, 2010. 184. 6910-6919.	0.8	103

#	Article	IF	CITATIONS
109	Perturbations in the surface structure of A22 Iraq foot-and-mouth disease virus accompanying coupled changes in host cell specificity and antigenicity. Structure, 1996, 4, 135-145.	3.3	100
110	Quantitative SARS-CoV-2 anti-spike responses to Pfizer–BioNTech and Oxford–AstraZeneca vaccines by previous infection status. Clinical Microbiology and Infection, 2021, 27, 1516.e7-1516.e14.	6.0	100
111	Crystal Structures of HIV-1 Reverse Transcriptase in Complex with Carboxanilide Derivativesâ€,‡. Biochemistry, 1998, 37, 14394-14403.	2.5	97
112	Structure of Foot-and-mouth disease virus serotype A1061 alone and complexed with oligosaccharide receptor: receptor conservation in the face of antigenic variation. Journal of General Virology, 2005, 86, 1909-1920.	2.9	95
113	A plate-based high-throughput assay for virus stability and vaccine formulation. Journal of Virological Methods, 2012, 185, 166-170.	2.1	94
114	The Crystal Structure of ORF-9b, a Lipid Binding Protein from the SARS Coronavirus. Structure, 2006, 14, 1157-1165.	3.3	91
115	Plant-made polio type 3 stabilized VLPs—a candidate synthetic polio vaccine. Nature Communications, 2017, 8, 245.	12.8	91
116	Hepatitis B small surface antigen particles are octahedral. Proceedings of the National Academy of Sciences of the United States of America, 2005, 102, 14783-14788.	7.1	90
117	How baculovirus polyhedra fit square pegs into round holes to robustly package viruses. EMBO Journal, 2010, 29, 505-514.	7.8	90
118	Dimeric Architecture of the Hendra Virus Attachment Glycoprotein: Evidence for a Conserved Mode of Assembly. Journal of Virology, 2010, 84, 6208-6217.	3.4	90
119	The crystal structure of coxsackievirus A9: new insights into the uncoating mechanisms of enteroviruses. Structure, 1999, 7, 1527-1538.	3.3	89
120	Structure-based energetics of protein interfaces guides foot-and-mouth disease virus vaccine design. Nature Structural and Molecular Biology, 2015, 22, 788-794.	8.2	89
121	More-powerful virus inhibitors from structure-based analysis of HEV71 capsid-binding molecules. Nature Structural and Molecular Biology, 2014, 21, 282-288.	8.2	88
122	Anti-spike antibody response to natural SARS-CoV-2 infection in the general population. Nature Communications, 2021, 12, 6250.	12.8	88
123	Design of Non-Nucleoside Inhibitors of HIV-1 Reverse Transcriptase with Improved Drug Resistance Properties. 1 Journal of Medicinal Chemistry, 2004, 47, 5912-5922.	6.4	87
124	Structural Plasticity of Eph Receptor A4 Facilitates Cross-Class Ephrin Signaling. Structure, 2009, 17, 1386-1397.	3.3	86
125	Structure and binding kinetics of three different human CD1d–α-galactosylceramide–specific T cell receptors. Journal of Experimental Medicine, 2006, 203, 699-710.	8.5	85
126	The N-glycosidase mechanism of ribosome-inactivating proteins implied by crystal structures of α-momorcharin. Structure, 1994, 2, 7-16.	3.3	84

#	Article	IF	CITATIONS
127	Crystal structure of the human p58 killer cell inhibitory receptor (KIR2DL3) specific for HLA-Cw3-related MHC class I. Structure, 1999, 7, 391-398.	3.3	84
128	αVβ6 Is a Novel Receptor for Human Fibrillin-1. Journal of Biological Chemistry, 2007, 282, 6743-6751.	3.4	83
129	Outrunning free radicals in room-temperature macromolecular crystallography. Acta Crystallographica Section D: Biological Crystallography, 2012, 68, 810-818.	2.5	83
130	Bluetongue virus VP4 is an RNA-capping assembly line. Nature Structural and Molecular Biology, 2007, 14, 449-451.	8.2	82
131	Structure of pyruvate kinase and similarities with other enzymes: possible implications for protein taxonomy and evolution. Nature, 1978, 271, 626-630.	27.8	81
132	The Structure of an RNAi Polymerase Links RNA Silencing and Transcription. PLoS Biology, 2006, 4, e434.	5.6	80
133	The structures of the neurotrophin 4 homodimer and the brainâ€derived neurotrophic factor/neurotrophin 4 heterodimer reveal a common Trkâ€binding site. Protein Science, 1999, 8, 2589-2597.	7.6	78
134	Insights into the Evolution of a Complex Virus from the Crystal Structure of Vaccinia Virus D13. Structure, 2011, 19, 1011-1020.	3.3	78
135	Lysosome sorting of β-glucocerebrosidase by LIMP-2 is targeted by the mannose 6-phosphate receptor. Nature Communications, 2014, 5, 4321.	12.8	78
136	Incorporation of tetanus-epitope into virus-like particles achieves vaccine responses even in older recipients in models of psoriasis, Alzheimer's and cat allergy. Npj Vaccines, 2017, 2, 30.	6.0	78
137	Structural comparison of two strains of foot-and-mouth disease virus subtype O1 and a laboratory antigenic variant, G67. Structure, 1995, 3, 571-580.	3.3	77
138	Implications for viral uncoating from the structure of bovine enterovirus. Nature Structural and Molecular Biology, 1995, 2, 224-231.	8.2	77
139	Crystal Structures of Penicillin-Binding Protein 3 from Pseudomonas aeruginosa: Comparison of Native and Antibiotic-Bound Forms. Journal of Molecular Biology, 2011, 405, 173-184.	4.2	77
140	2-Amino-6-arylsulfonylbenzonitriles as Non-nucleoside Reverse Transcriptase Inhibitors of HIV-1. Journal of Medicinal Chemistry, 2001, 44, 1866-1882.	6.4	75
141	High-resolution structure of the catalytic region of MICAL (molecule interacting with CasL), a multidomain flavoenzyme-signaling molecule. Proceedings of the National Academy of Sciences of the United States of America, 2005, 102, 16836-16841.	7.1	75
142	Rules of engagement between αvβ6 integrin and foot-and-mouth disease virus. Nature Communications, 2017, 8, 15408.	12.8	75
143	Inhibition of Apoptosis and NF-κB Activation by Vaccinia Protein N1 Occur via Distinct Binding Surfaces and Make Different Contributions to Virulence. PLoS Pathogens, 2011, 7, e1002430.	4.7	73
144	Unexpected mode of engagement between enterovirus 71 and its receptor SCARB2. Nature Microbiology, 2019, 4, 414-419.	13.3	73

#	Article	IF	CITATIONS
145	3D Correlative Cryo-Structured Illumination Fluorescence and Soft X-ray Microscopy Elucidates Reovirus Intracellular Release Pathway. Cell, 2020, 182, 515-530.e17.	28.9	73
146	Unexpected structure for the N-terminal domain of hepatitis C virus envelope glycoprotein E1. Nature Communications, 2014, 5, 4874.	12.8	72
147	Exploiting fast detectors to enter a new dimension in room-temperature crystallography. Acta Crystallographica Section D: Biological Crystallography, 2014, 70, 1248-1256.	2.5	72
148	Low-dose phase retrieval of biological specimens using cryo-electron ptychography. Nature Communications, 2020, 11, 2773.	12.8	72
149	3′-Azido-3′-deoxythymidine drug resistance mutations in HIV-1 reverse transcriptase can induce long range conformational changes. Proceedings of the National Academy of Sciences of the United States of America, 1998, 95, 9518-9523.	7.1	71
150	Rhabdovirus Matrix Protein Structures Reveal a Novel Mode of Self-Association. PLoS Pathogens, 2008, 4, e1000251.	4.7	71
151	Unusual Molecular Architecture of the Machupo Virus Attachment Glycoprotein. Journal of Virology, 2009, 83, 8259-8265.	3.4	71
152	Fixed target combined with spectral mapping: approaching 100% hit rates for serial crystallography. Acta Crystallographica Section D: Structural Biology, 2016, 72, 944-955.	2.3	71
153	Machining protein microcrystals for structure determination by electron diffraction. Proceedings of the National Academy of Sciences of the United States of America, 2018, 115, 9569-9573.	7.1	69
154	A Similar Pattern of Interaction for Different Antibodies with a Major Antigenic Site of Foot-and-Mouth Disease Virus: Implications for Intratypic Antigenic Variation. Journal of Virology, 1998, 72, 739-748.	3.4	69
155	Determination of the Affinity and Kinetic Constants for the Interaction between the Human Virus Echovirus 11 and Its Cellular Receptor, CD55. Journal of Biological Chemistry, 1998, 273, 30443-30447.	3.4	68
156	Nonstandard Peptide Binding Revealed by Crystal Structures of HLA-B*5101 Complexed with HIV Immunodominant Epitopes. Journal of Immunology, 2000, 165, 3260-3267.	0.8	68
157	Carbohydrate and Domain Architecture of an Immature Antibody Glycoform Exhibiting Enhanced Effector Functions. Journal of Molecular Biology, 2009, 387, 1061-1066.	4.2	67
158	The Structure of the Macrophage Signal Regulatory Protein α (SIRPα) Inhibitory Receptor Reveals a Binding Face Reminiscent of That Used by T Cell Receptors. Journal of Biological Chemistry, 2007, 282, 14567-14575.	3.4	66
159	Structure and Function of A41, a Vaccinia Virus Chemokine Binding Protein. PLoS Pathogens, 2008, 4, e5.	4.7	66
160	How vaccinia virus has evolved to subvert the host immune response. Journal of Structural Biology, 2011, 175, 127-134.	2.8	66
161	Target Identification and Mode of Action of Four Chemically Divergent Drugs against Ebolavirus Infection. Journal of Medicinal Chemistry, 2018, 61, 724-733.	6.4	66
162	Chemical and Structural Analysis of an Antibody Folding Intermediate Trapped during Glycan Biosynthesis. Journal of the American Chemical Society, 2012, 134, 17554-17563.	13.7	65

#	Article	IF	CITATIONS
163	The structure of CrgA from Neisseria meningitidis reveals a new octameric assembly state for LysR transcriptional regulators. Nucleic Acids Research, 2009, 37, 4545-4558.	14.5	64
164	Equine Rhinitis A Virus and Its Low pH Empty Particle: Clues Towards an Aphthovirus Entry Mechanism?. PLoS Pathogens, 2009, 5, e1000620.	4.7	64
165	An Observational Cohort Study on the Incidence of Severe Acute Respiratory Syndrome Coronavirus 2 (SARS-CoV-2) Infection and B.1.1.7 Variant Infection in Healthcare Workers by Antibody and Vaccination Status. Clinical Infectious Diseases, 2022, 74, 1208-1219.	5.8	64
166	Design of Non-nucleoside Inhibitors of HIV-1 Reverse Transcriptase with Improved Drug Resistance Properties. 2 Journal of Medicinal Chemistry, 2004, 47, 5923-5936.	6.4	61
167	Antigenic Switching of Hepatitis B Virus by Alternative Dimerization of the Capsid Protein. Structure, 2013, 21, 133-142.	3.3	61
168	A revised partiality model and post-refinement algorithm for X-ray free-electron laser data. Acta Crystallographica Section D: Biological Crystallography, 2015, 71, 1400-1410.	2.5	60
169	Ligand Binding by the Immunoglobulin Superfamily Recognition Molecule CD2 Is Glycosylation-independent. Journal of Biological Chemistry, 1995, 270, 369-375.	3.4	59
170	Multiple liquid crystalline geometries of highly compacted nucleic acid in a dsRNA virus. Nature, 2019, 570, 252-256.	27.8	59
171	Structures of Coxsackievirus A16 Capsids with Native Antigenicity: Implications for Particle Expansion, Receptor Binding, and Immunogenicity. Journal of Virology, 2015, 89, 10500-10511.	3.4	58
172	A Tick Protein with a Modified Kunitz Fold Inhibits Human Tryptase. Journal of Molecular Biology, 2007, 368, 1172-1186.	4.2	57
173	CryoSIM: super-resolution 3D structured illumination cryogenic fluorescence microscopy for correlated ultrastructural imaging. Optica, 2020, 7, 802.	9.3	57
174	New methods for indexing multi-lattice diffraction data. Acta Crystallographica Section D: Biological Crystallography, 2014, 70, 2652-2666.	2.5	56
175	Structure of CPV17 polyhedrin determined by the improved analysis of serial femtosecond crystallographic data. Nature Communications, 2015, 6, 6435.	12.8	56
176	Using Structural Information to Change the Phosphotransfer Specificity of a Two-Component Chemotaxis Signalling Complex. PLoS Biology, 2010, 8, e1000306.	5.6	55
177	Automation of large scale transient protein expression in mammalian cells. Journal of Structural Biology, 2011, 175, 209-215.	2.8	55
178	Expression of soluble recombinant glycoproteins with predefined glycosylation: application to the crystallization of the T-cell glycoprotein CD2. Protein Engineering, Design and Selection, 1993, 6, 229-232.	2.1	54
179	Site-Specific Steric Control of SARS-CoV-2 Spike Glycosylation. Biochemistry, 2021, 60, 2153-2169.	2.5	54
180	Where is crystallography going?. Acta Crystallographica Section D: Structural Biology, 2018, 74, 152-166.	2.3	54

#	Article	IF	CITATIONS
181	Flexibility of the Major Antigenic Loop of Foot-and-Mouth Disease Virus Bound to a Fab Fragment of a Neutralising Antibody: Structure and Neutralisation. Virology, 1999, 255, 260-268.	2.4	53
182	Atomic Resolution Structure of Moloney Murine Leukemia Virus Matrix Protein and Its Relationship to Other Retroviral Matrix Proteins. Structure, 2002, 10, 1627-1636.	3.3	53
183	Crystal structure of the Murray Valley encephalitis virus NS5 methyltransferase domain in complex with cap analogues. Journal of General Virology, 2007, 88, 2228-2236.	2.9	52
184	The antibody response to SARS-CoV-2 Beta underscores the antigenic distance to other variants. Cell Host and Microbe, 2022, 30, 53-68.e12.	11.0	52
185	Efficient production of foot-and-mouth disease virus empty capsids in insect cells following down regulation of 3C protease activity. Journal of Virological Methods, 2013, 187, 406-412.	2.1	51
186	Building meaningful models of glycoproteins. Nature Structural and Molecular Biology, 2007, 14, 354-354.	8.2	48
187	Structural explanation for the role of Mn2+ in the activity of ϕ6 RNA-dependent RNA polymerase. Nucleic Acids Research, 2008, 36, 6633-6644.	14.5	48
188	Mapping the lκB Kinase β (IKKβ)-binding Interface of the B14 Protein, a Vaccinia Virus Inhibitor of IKKβ-mediated Activation of Nuclear Factor κB. Journal of Biological Chemistry, 2011, 286, 20727-20735.	3.4	48
189	Determination of the Structure of a Decay Accelerating Factor-Binding Clinical Isolate of Echovirus 11 Allows Mapping of Mutants with Altered Receptor Requirements for Infection. Journal of Virology, 2002, 76, 7694-7704.	3.4	46
190	Potential long-term effects of SARS-CoV-2 infection on the pulmonary vasculature: a global perspective. Nature Reviews Cardiology, 2022, 19, 314-331.	13.7	46
191	Plate Tectonics of Virus Shell Assembly and Reorganization in Phage Φ8, a Distant Relative of Mammalian Reoviruses. Structure, 2013, 21, 1384-1395.	3.3	45
192	Virus found in a boreal lake links ssDNA and dsDNA viruses. Proceedings of the National Academy of Sciences of the United States of America, 2017, 114, 8378-8383.	7.1	44
193	A critical evaluation of the predicted and X-ray structures of ?-Lactalbumin. The Protein Journal, 1990, 9, 549-563.	1.1	43
194	Structure of CrmE, a Virus-encoded Tumour Necrosis Factor Receptor. Journal of Molecular Biology, 2007, 372, 660-671.	4.2	43
195	Structure of Ljungan virus provides insight into genome packaging of this picornavirus. Nature Communications, 2015, 6, 8316.	12.8	43
196	Crystallographic Analysis of the Binding Modes of Thiazoloisoindolinone Non-Nucleoside Inhibitors to HIV-1 Reverse Transcriptase and Comparison with Modeling Studies. Journal of Medicinal Chemistry, 1999, 42, 3845-3851.	6.4	42
197	The Structural Basis for RNA Specificity and Ca2+ Inhibition of an RNA-Dependent RNA Polymerase. Structure, 2004, 12, 307-316.	3.3	42
198	Benefits of Automated Crystallization Plate Tracking, Imaging, and Analysis. Structure, 2005, 13, 175-182.	3.3	42

#	Article	IF	CITATIONS
199	An Ion-channel Modulator from the Saliva of the Brown Ear Tick has a Highly Modified Kunitz/BPTI Structure. Journal of Molecular Biology, 2009, 389, 734-747.	4.2	42
200	Automatic comparison and classification of protein structures. Journal of Structural Biology, 2013, 183, 47-56.	2.8	42
201	Potent neutralization of hepatitis A virus reveals a receptor mimic mechanism and the receptor recognition site. Proceedings of the National Academy of Sciences of the United States of America, 2017, 114, 770-775.	7.1	42
202	Automated Structural Comparisons Clarify the Phylogeny of the Right-Hand-Shaped Polymerases. Molecular Biology and Evolution, 2014, 31, 2741-2752.	8.9	41
203	Rigid-body Ligand Recognition Drives Cytotoxic T-lymphocyte Antigen 4 (CTLA-4) Receptor Triggering. Journal of Biological Chemistry, 2011, 286, 6685-6696.	3.4	39
204	<i>In cellulo</i> structure determination of a novel cypovirus polyhedrin. Acta Crystallographica Section D: Biological Crystallography, 2014, 70, 1435-1441.	2.5	39
205	Structure of glycosylated <scp>NPC</scp> 1 luminal domain C reveals insights into <scp>NPC</scp> 2 and Ebola virus interactions. FEBS Letters, 2016, 590, 605-612.	2.8	39
206	Structure of Equine Infectious Anemia Virus Matrix Protein. Journal of Virology, 2002, 76, 1876-1883.	3.4	38
207	Bacteriophage P23-77 Capsid Protein Structures Reveal the Archetype of an Ancient Branch from a Major Virus Lineage. Structure, 2013, 21, 718-726.	3.3	38
208	Structures of Ebola Virus Glycoprotein Complexes with Tricyclic Antidepressant and Antipsychotic Drugs. Journal of Medicinal Chemistry, 2018, 61, 4938-4945.	6.4	38
209	Effects of <i>N</i> â€butyldeoxynojirimycin and the Lec3.2.8.1 mutant phenotype on Nâ€glycan processing in Chinese hamster ovary cells: Application to glycoprotein crystallization. Protein Science, 1999, 8, 1696-1701.	7.6	37
210	Evaluation and Use of In-Silico Structure-Based Epitope Prediction with Foot-and-Mouth Disease Virus. PLoS ONE, 2013, 8, e61122.	2.5	37
211	The structure of a prokaryotic viral envelope protein expands the landscape of membrane fusion proteins. Nature Communications, 2019, 10, 846.	12.8	37
212	Diffraction quality crystals of PRD1, a 66-MDa dsDNA virus with an internal membrane. Journal of Structural Biology, 2002, 139, 103-112.	2.8	36
213	Structure of human Aichi virus and implications for receptor binding. Nature Microbiology, 2016, 1, 16150.	13.3	36
214	Assembly intermediates of orthoreovirus captured in the cell. Nature Communications, 2020, 11, 4445.	12.8	36
215	Models Which Explain the Inhibition of Reverse Transcriptase by HIV-1-Specific (Thio)carboxanilide Derivatives1. Biochemical and Biophysical Research Communications, 1997, 234, 458-464.	2.1	35
216	The Structure and Function of the Outer Coat Protein VP9 of Banna Virus. Structure, 2005, 13, 17-28.	3.3	35

13

#	Article	IF	CITATIONS
217	A Human Embryonic Kidney 293T Cell Line Mutated at the Golgi α-Mannosidase II Locus. Journal of Biological Chemistry, 2009, 284, 21684-21695.	3.4	35
218	Structure of Signal-regulatory Protein α. Journal of Biological Chemistry, 2009, 284, 26613-26619.	3.4	35
219	<i>TakeTwo</i> : an indexing algorithm suited to still images with known crystal parameters. Acta Crystallographica Section D: Structural Biology, 2016, 72, 956-965.	2.3	35
220	The democratization of cryo-EM. Nature Methods, 2016, 13, 607-608.	19.0	35
221	Double-stranded RNA virus outer shell assembly by bona fide domain-swapping. Nature Communications, 2017, 8, 14814.	12.8	35
222	Structures of orbivirus VP7: implications for the role of this protein in the viral life cycle. Structure, 1997, 5, 871-883.	3.3	34
223	Lipofectin increases the specific activity of cypovirus particles for cultured insect cells. Journal of Virological Methods, 1999, 78, 177-189.	2.1	34
224	Shared paramyxoviral glycoprotein architecture is adapted for diverse attachment strategies. Biochemical Society Transactions, 2010, 38, 1349-1355.	3.4	34
225	The N-Terminus of the RNA Polymerase from Infectious Pancreatic Necrosis Virus Is the Determinant of Genome Attachment. PLoS Pathogens, 2011, 7, e1002085.	4.7	34
226	Structure-Based in Silico Screening Identifies a Potent Ebolavirus Inhibitor from a Traditional Chinese Medicine Library. Journal of Medicinal Chemistry, 2019, 62, 2928-2937.	6.4	34
227	Production and crystallization of MHC class I B allele single peptide complexes. FEBS Letters, 1996, 383, 119-123.	2.8	33
228	Crystal Structure and Binding Properties of the CD2 and CD244 (2B4)-binding Protein, CD48. Journal of Biological Chemistry, 2006, 281, 29309-29320.	3.4	33
229	Pushing the limits of sulfur SAD phasing: <i>de novo</i> structure solution of the N-terminal domain of the ectodomain of HCV E1. Acta Crystallographica Section D: Biological Crystallography, 2014, 70, 2197-2203.	2.5	33
230	Production, crystallization, and preliminary Xâ€ray analysis of the human MHC class Ib molecule HLAâ€E. Protein Science, 1998, 7, 1264-1266.	7.6	32
231	Semi-automated microseeding of nanolitre crystallization experiments. Acta Crystallographica Section F: Structural Biology Communications, 2008, 64, 14-18.	0.7	31
232	Noncatalytic Ions Direct the RNA-Dependent RNA Polymerase of Bacterial Double-Stranded RNA Virus ϕ6 from <i>De Novo</i> Initiation to Elongation. Journal of Virology, 2012, 86, 2837-2849.	3.4	31
233	The Human Otubain2-Ubiquitin Structure Provides Insights into the Cleavage Specificity of Poly-Ubiquitin-Linkages. PLoS ONE, 2015, 10, e0115344.	2.5	31
234	Redundant Late Domain Functions of Tandem VP2 YPX ₃ L Motifs in Nonlytic Cellular Egress of Quasi-enveloped Hepatitis A Virus. Journal of Virology, 2018, 92, .	3.4	31

#	Article	IF	CITATIONS
235	Crystallization and preliminary X-ray diffraction analysis of foot-and-mouth disease virus. Journal of Molecular Biology, 1987, 196, 591-597.	4.2	30
236	Structure of the Murray Valley encephalitis virus RNA helicase at 1.9 Ã resolution. Protein Science, 2007, 16, 2294-2300.	7.6	30
237	Structural Basis of Mechanochemical Coupling in a Hexameric Molecular Motor. Journal of Biological Chemistry, 2008, 283, 3607-3617.	3.4	30
238	Characterization of epitope-tagged foot-and-mouth disease virus. Journal of General Virology, 2012, 93, 2371-2381.	2.9	30
239	Seneca Valley virus attachment and uncoating mediated by its receptor anthrax toxin receptor 1. Proceedings of the National Academy of Sciences of the United States of America, 2018, 115, 13087-13092.	7.1	30
240	Cells under siege: Viral glycoprotein interactions at the cell surface. Journal of Structural Biology, 2011, 175, 120-126.	2.8	29
241	Models of the three-dimensional structures of echidna, horse, and pigeon lysozymes: Calcium-binding lysozymes and their relationship with α-lactalbumins. The Protein Journal, 1994, 13, 569-584.	1.1	28
242	Utility of recombinant integrin αvβ6 as a capture reagent in immunoassays for the diagnosis of foot-and-mouth disease. Journal of Virological Methods, 2005, 127, 69-79.	2.1	28
243	Back-priming mode of ï•6 RNA-dependent RNA polymerase. Journal of General Virology, 2005, 86, 521-526.	2.9	28
244	Generation and Characterization of a Chimeric Rabbit/Human Fab for Co-Crystallization of HIV-1 Rev. Journal of Molecular Biology, 2010, 397, 697-708.	4.2	28
245	SAT2 Foot-and-Mouth Disease Virus Structurally Modified for Increased Thermostability. Journal of Virology, 2017, 91, .	3.4	28
246	Atomic structure of the Epstein-Barr virus portal. Nature Communications, 2019, 10, 3891.	12.8	28
247	Hand-foot-and-mouth disease virus receptor KREMEN1 binds the canyon of Coxsackie Virus A10. Nature Communications, 2020, 11, 38.	12.8	28
248	On the release of <i>cppxfel</i> for processing X-ray free-electron laser images. Journal of Applied Crystallography, 2016, 49, 1065-1072.	4.5	28
249	Expression cloning of an equine T-lymphocyte glycoprotein CD2 cDNA. Structure-based analysis of conserved sequence elements. FEBS Journal, 1994, 219, 969-976.	0.2	27
250	Design of a data model for developing laboratory information management and analysis systems for protein production. Proteins: Structure, Function and Bioinformatics, 2004, 58, 278-284.	2.6	27
251	Crystal lattice as biological phenotype for insect viruses. Protein Science, 2005, 14, 2741-2743.	7.6	26
252	Neutralization Mechanisms of Two Highly Potent Antibodies against Human Enterovirus 71. MBio, 2018, 9, .	4.1	26

#	Article	IF	CITATIONS
253	Crystal Structure of Swine Vesicular Disease Virus and Implications for Host Adaptation. Journal of Virology, 2003, 77, 5475-5486.	3.4	25
254	Polyhedra structures and the evolution of the insect viruses. Journal of Structural Biology, 2015, 192, 88-99.	2.8	25
255	Cutting complexity down to size. Nature, 1997, 386, 437-438.	27.8	24
256	Bispecific repurposed medicines targeting the viral and immunological arms of COVID-19. Scientific Reports, 2021, 11, 13208.	3.3	24
257	Electron Bio-Imaging Centre (eBIC): the UK national research facility for biological electron microscopy. Acta Crystallographica Section D: Structural Biology, 2017, 73, 488-495.	2.3	24
258	Crystallization and preliminary X-ray analysis of three serotypes of foot-and-mouth disease virus. Journal of Molecular Biology, 1992, 228, 1263-1268.	4.2	23
259	Gene silencing pathway RNA-dependent RNA polymerase of Neurospora crassa: yeast expression and crystallization of selenomethionated QDE-1 protein. Journal of Structural Biology, 2005, 149, 111-115.	2.8	23
260	Binding of (5 <i>S</i>)-Penicilloic Acid to Penicillin Binding Protein 3. ACS Chemical Biology, 2013, 8, 2112-2116.	3.4	23
261	Tracking in atomic detail the functional specializations in viral RecA helicases that occur during evolution. Nucleic Acids Research, 2013, 41, 9396-9410.	14.5	23
262	Stringent thresholds in SARS-CoV-2 IgG assays lead to under-detection of mild infections. BMC Infectious Diseases, 2021, 21, 187.	2.9	23
263	Mammalian expression of virus-like particles as a proof of principle for next generation polio vaccines. Npj Vaccines, 2021, 6, 5.	6.0	23
264	Time-resolved structural studies on catalysis in the crystal with glycogen phosphorylase b. Biochemical Society Transactions, 1986, 14, 538-541.	3.4	22
265	Characterizing sequence variation in the VP1 capsid proteins of foot and mouth disease virus (serotype 0) with respect to virion structure. Journal of Molecular Evolution, 1998, 46, 465-475.	1.8	22
266	Virus Crystallography. Molecular Biotechnology, 1999, 12, 13-24.	2.4	22
267	Crystal structure of a 3â€oxoacylâ€(acylcarrier protein) reductase (BA3989) from <i>Bacillus anthracis</i> at 2.4â€Ã resolution. Proteins: Structure, Function and Bioinformatics, 2008, 70, 562-567.	2.6	22
268	Insights into the pre-initiation events of bacteriophage φ6 RNA-dependent RNA polymerase: towards the assembly of a productive binary complex. Nucleic Acids Research, 2009, 37, 1182-1192.	14.5	22
269	The structure of a reduced form of OxyR from Neisseria meningitidis. BMC Structural Biology, 2010, 10, 10.	2.3	22
270	Potent antiviral agents fail to elicit genetically-stable resistance mutations in either enterovirus 71 or Coxsackievirus A16. Antiviral Research, 2015, 124, 77-82.	4.1	22

#	Article	IF	CITATIONS
271	A national facility for biological cryo-electron microscopy. Acta Crystallographica Section D: Biological Crystallography, 2015, 71, 127-135.	2.5	22
272	The Structure of HIV-1 Rev Filaments Suggests a Bilateral Model for Rev-RRE Assembly. Structure, 2016, 24, 1068-1080.	3.3	22
273	Docking mission accomplished. Nature, 1994, 371, 19-20.	27.8	21
274	Recognition surfaces of MHC class I. Immunological Reviews, 1998, 163, 121-128.	6.0	21
275	Reconfiguration of yeast 40S ribosomal subunit domains by the translation initiation multifactor complex. Proceedings of the National Academy of Sciences of the United States of America, 2007, 104, 5788-5793.	7.1	21
276	Structures of foot and mouth disease virus pentamers: Insight into capsid dissociation and unexpected pentamer reassociation. PLoS Pathogens, 2017, 13, e1006607.	4.7	21
277	Crystallization and preliminary X-ray crystallographic studies on the bacteriophage Φ6 RNA-dependent RNA polymerase. Acta Crystallographica Section D: Biological Crystallography, 2000, 56, 1473-1475.	2.5	20
278	Macromolecular assemblies: greater than their parts. Current Opinion in Structural Biology, 2001, 11, 107-113.	5.7	20
279	The Mechanics of Translocation: A Molecular "Spring-and-Ratchet―System. Structure, 2008, 16, 664-672.	3.3	20
280	Structure Elucidation of Coxsackievirus A16 in Complex with GPP3 Informs a Systematic Review of Highly Potent Capsid Binders to Enteroviruses. PLoS Pathogens, 2015, 11, e1005165.	4.7	20
281	Uridine(5')diphospho(1)-alpha-d-glucose. A binding study to glycogen phosphorylase b in the crystal. FEBS Journal, 1988, 173, 569-578.	0.2	19
282	The structure of foot-and-mouth disease virus: implications for its physical and biological properties. Veterinary Microbiology, 1990, 23, 21-34.	1.9	19
283	Specific Interactions between Human Integrin αvβ3and Chimeric Hepatitis B Virus Core Particles Bearing the Receptor-Binding Epitope of Foot-and-Mouth Disease Virus. Virology, 1997, 239, 150-157.	2.4	19
284	Functional characteristics of HIV-1 subtype C compatible with increased heterosexual transmissibility. Aids, 2009, 23, 1047-1057.	2.2	19
285	Disruption of α-mannosidase processing induces non-canonical hybrid-type glycosylation. FEBS Letters, 2007, 581, 1963-1968.	2.8	18
286	Domain Metastability: A Molecular Basis for Immunoglobulin Deposition?. Journal of Molecular Biology, 2010, 399, 207-213.	4.2	18
287	The Protein Information Management System (PiMS): a generic tool for any structural biology research laboratory. Acta Crystallographica Section D: Biological Crystallography, 2011, 67, 249-260.	2.5	18
288	Hepatitis A Virus Capsid Structure. Cold Spring Harbor Perspectives in Medicine, 2019, 9, a031807.	6.2	18

#	Article	IF	CITATIONS
289	Application of In Situ Diffraction in High-Throughput Structure Determination Platforms. Methods in Molecular Biology, 2015, 1261, 233-253.	0.9	18
290	Crystallization and functional analysis of a soluble deglycosylated form of the human costimulatory molecule B7-1. Acta Crystallographica Section D: Biological Crystallography, 2001, 57, 605-608.	2.5	17
291	Expression, purification and crystallization of a lyssavirus matrix (M) protein. Acta Crystallographica Section F: Structural Biology Communications, 2008, 64, 258-262.	0.7	17
292	Use of the α-mannosidase I inhibitor kifunensine allows the crystallization of apo CTLA-4 homodimer produced in long-term cultures of Chinese hamster ovary cells. Acta Crystallographica Section F: Structural Biology Communications, 2011, 67, 785-789.	0.7	17
293	Crystal structures of penicillinâ€binding protein 3 in complexes with azlocillin and cefoperazone in both acylated and deacylated forms. FEBS Letters, 2016, 590, 288-297.	2.8	17
294	Assembly of complex viruses exemplified by a halophilic euryarchaeal virus. Nature Communications, 2019, 10, 1456.	12.8	17
295	What Does it Take to Make a Virus: The Concept of the Viral 'Self'. , 2010, , 35-58.		17
296	SARS-CoV-2 antibody prevalence, titres and neutralising activity in an antenatal cohort, United Kingdom, 14 April to 15 June 2020. Eurosurveillance, 2020, 25, .	7.0	17
297	Structures of an alanine racemase from <i>Bacillus anthracis</i> (BA0252) in the presence and absence of (<i>R</i>)-1-aminoethylphosphonic acid (<scp>L</scp> -Ala-P). Acta Crystallographica Section F: Structural Biology Communications, 2008, 64, 327-333.	0.7	16
298	Crystallization and preliminary X-ray analysis of CrgA, a LysR-type transcriptional regulator from pathogenicNeisseria meningitidisMC58. Acta Crystallographica Section F: Structural Biology Communications, 2008, 64, 797-801.	0.7	16
299	Glutathione facilitates enterovirus assembly by binding at a druggable pocket. Communications Biology, 2020, 3, 9.	4.4	16
300	Structure of a VP1-VP3 Complex Suggests How Birnaviruses Package the VP1 Polymerase. Journal of Virology, 2013, 87, 3229-3236.	3.4	15
301	Weissenberg data collection for macromolecular crystallography. Current Opinion in Structural Biology, 1993, 3, 737-740.	5.7	14
302	Recognition at the cell surface: recent structural insights. Current Opinion in Structural Biology, 1995, 5, 735-743.	5.7	14
303	Complementing crystallography: the role of cryo-electron microscopy in structural biology. Acta Crystallographica Section D: Biological Crystallography, 1999, 55, 1742-1749.	2.5	14
304	In Vitro Activities of the Multifunctional RNA Silencing Polymerase QDE-1 of Neurospora crassa*. Journal of Biological Chemistry, 2010, 285, 29367-29374.	3.4	14
305	A RANKL mutant used as an inter-species vaccine for efficient immunotherapy of osteoporosis. Scientific Reports, 2015, 5, 14150.	3.3	14
306	Production, crystallization and preliminary X-ray crystallographic studies of the bacteriophage ï•12 packaging motor. Acta Crystallographica Section D: Biological Crystallography, 2004, 60, 588-590.	2.5	13

#	Article	IF	CITATIONS
307	The Crystal Structure of UMP Kinase from Bacillus anthracis (BA1797) Reveals an Allosteric Nucleotide-Binding Site. Journal of Molecular Biology, 2008, 381, 1098-1105.	4.2	13
308	Some lessons from the systematic production and structural analysis of soluble αβ T-cell receptors. Journal of Immunological Methods, 2009, 350, 14-21.	1.4	13
309	Crystal structure of equine rhinitis A virus in complex with its sialic acid receptor. Journal of General Virology, 2010, 91, 1971-1977.	2.9	13
310	The Tandem Zinc-Finger Region of Human ZHX Adopts a Novel C2H2 Zinc Finger Structure with a C-Terminal Extension. Biochemistry, 2009, 48, 4431-4439.	2.5	12
311	Diamond Light Source: status and perspectives. Philosophical Transactions Series A, Mathematical, Physical, and Engineering Sciences, 2015, 373, 20130161.	3.4	12
312	Viral envelope glycoproteins swing into action. Structure, 1995, 3, 645-648.	3.3	11
313	Model of the equine rhinitis A virus capsid: identification of a major neutralizing immunogenic site. Journal of General Virology, 2003, 84, 2365-2373.	2.9	11
314	Structure of 5-formyltetrahydrofolate cyclo-ligase fromBacillus anthracis(BA4489). Acta Crystallographica Section F: Structural Biology Communications, 2007, 63, 168-172.	0.7	11
315	From lows to highs: using low-resolution models to phase X-ray data. Acta Crystallographica Section D: Biological Crystallography, 2013, 69, 2257-2265.	2.5	11
316	Towards in cellulo virus crystallography. Scientific Reports, 2018, 8, 3771.	3.3	11
317	Chimeric O1K foot-and-mouth disease virus with SAT2 outer capsid as an FMD vaccine candidate. Scientific Reports, 2018, 8, 13654.	3.3	11
318	The role of the light chain in the structure and binding activity of two cattle antibodies that neutralize bovine respiratory syncytial virus. Molecular Immunology, 2019, 112, 123-130.	2.2	11
319	Structural and functional analysis of protective antibodies targeting the threefold plateau of enterovirus 71. Nature Communications, 2020, 11, 5253.	12.8	11
320	Preliminary Crystallographic Analysis of Bovine Enterovirus. Journal of Molecular Biology, 1993, 231, 930-932.	4.2	10
321	SPINE: Structural Proteomics IN Europe – the best of both worlds. Acta Crystallographica Section D: Biological Crystallography, 2006, 62, ii-i.	2.5	10
322	Crystal structure of signal regulatory protein gamma (SIRPγ) in complex with an antibody Fab fragment. BMC Structural Biology, 2013, 13, 13.	2.3	10
323	Cloning, expression, purification, and crystallisation of HIV-2 reverse transcriptase. Protein Expression and Purification, 2003, 27, 12-18.	1.3	9
324	Preliminary crystallographic analysis of the major capsid protein P2 of the lipid-containing bacteriophage PM2. Acta Crystallographica Section F: Structural Biology Communications, 2005, 61, 762-765.	0.7	9

#	Article	IF	CITATIONS
325	Selenomethionine labeling of large biological macromolecular complexes: Probing the structure of marine bacterial virus PM2. Journal of Structural Biology, 2008, 161, 204-210.	2.8	9
326	The C-terminal priming domain is strongly associated with the main body of bacteriophage ϕ6 RNA-dependent RNA polymerase. Virology, 2012, 432, 184-193.	2.4	9
327	Crystallization and X-ray Diffraction Study of Recombinant Platelet-derived Endothelial Cell Growth Factor. Journal of Molecular Biology, 1993, 234, 879-880.	4.2	8
328	xtalPiMS: A PiMS-based web application for the management and monitoring of crystallization trials. Journal of Structural Biology, 2011, 175, 230-235.	2.8	8
329	Crystallization and preliminary crystallographic analysis of the major capsid proteins VP16 and VP17 of bacteriophage P23-77. Acta Crystallographica Section F: Structural Biology Communications, 2012, 68, 580-583.	0.7	8
330	Expression, purification and crystallization of the ectodomain of the envelope glycoprotein E2 fromBovine viral diarrhoea virus. Acta Crystallographica Section F: Structural Biology Communications, 2013, 69, 35-38.	0.7	8
331	Structure determination from a single high-pressure-frozen virus crystal. Acta Crystallographica Section D: Biological Crystallography, 2013, 69, 308-312.	2.5	8
332	Journey to the core of HIV. Nature Structural and Molecular Biology, 1996, 3, 818-820.	8.2	7
333	Recovery of data from perfectly twinned virus crystals revisited. Acta Crystallographica Section D: Structural Biology, 2016, 72, 817-822.	2.3	7
334	Structure of Cat Muscle Pyruvate Kinase at 0.26 nm Resolution. Biochemical Society Transactions, 1977, 5, 654-657.	3.4	6
335	Preliminary Crystallographic Analysis of Coxsackievirus A9. Journal of Molecular Biology, 1993, 230, 667-669.	4.2	6
336	Crystallization and Preliminary X-ray Investigation of Recombinant Simian Immunodeficiency Virus Matrix Protein. Journal of Molecular Biology, 1994, 241, 744-746.	4.2	6
337	Hybrid Vigor: Hybrid Methods In Viral Structure Determination. Advances in Protein Chemistry, 2003, 64, 37-91.	4.4	6
338	Overcoming the false-minima problem in direct methods: structure determination of the packaging enzyme P4 from bacteriophage I•13. Acta Crystallographica Section D: Biological Crystallography, 2005, 61, 1238-1244.	2.5	6
339	An idea whose time has come. Genome Biology, 2007, 8, 408.	9.6	6
340	Humidity control as a strategy for lattice optimization applied to crystals of HLA-A*1101 complexed with variant peptides from dengue virus. Acta Crystallographica Section F: Structural Biology Communications, 2007, 63, 386-392.	0.7	6
341	The use of low-resolution phasing followed by phase extension from 7.6 to 2.5â€Ã resolution with noncrystallographic symmetry to solve the structure of a bacteriophage capsid protein. Acta Crystallographica Section D: Biological Crystallography, 2011, 67, 228-232.	2.5	6
342	Diamond Light Source: contributions to SARS-CoV-2 biology and therapeutics. Biochemical and Biophysical Research Communications, 2021, 538, 40-46.	2.1	6

#	Article	IF	CITATIONS
343	Structures and therapeutic potential of anti-RBD human monoclonal antibodies against SARS-CoV-2. Theranostics, 2022, 12, 1-17.	10.0	6
344	Crystallization of human tumour necrosis factor. Journal of Crystal Growth, 1990, 100, 168-170.	1.5	5
345	HEPT: From an investigation of lithiation of nucleosides towards a rational design of non-nucleoside reverse transcriptase inhibitors of HIV-1. Advances in Antiviral Drug Design, 1999, , 93-144.	0.6	5
346	Going soft and SAD with manganese. Acta Crystallographica Section D: Biological Crystallography, 2005, 61, 108-111.	2.5	5
347	Structure determination of human semaphorin 4D as an example of the use of MAD in non-optimal cases. Acta Crystallographica Section D: Biological Crystallography, 2006, 62, 108-115.	2.5	5
348	The B Cell Response to Foot-and-Mouth Disease Virus in Cattle following Sequential Vaccination with Multiple Serotypes. Journal of Virology, 2017, 91, .	3.4	5
349	<i>SynchLink</i> : an iOS app for ISPyB. Journal of Applied Crystallography, 2014, 47, 1781-1783.	4.5	5
350	Imperfection and radiation damage in protein crystals studied with coherent radiation. Journal of Synchrotron Radiation, 2016, 23, 228-237.	2.4	5
351	The slip-and-slide algorithm: a refinement protocol for detector geometry. Journal of Synchrotron Radiation, 2017, 24, 1152-1162.	2.4	5
352	Scanning electron microscopy as a method for sample visualization in protein X-ray crystallography. IUCrJ, 2020, 7, 500-508.	2.2	5
353	Some problems in relation to the structures of insulin derivatives. Biochemical Society Transactions, 1983, 11, 419-425.	3.4	4
354	Large unit cells and cellular mechanics. Nature Structural Biology, 1998, 5, 630-634.	9.7	4
355	Crystallization and preliminary X-ray analysis of human rhinovirus serotype 2 (HRV2). Acta Crystallographica Section D: Biological Crystallography, 1999, 55, 1459-1461.	2.5	4
356	Order and disorder in crystals of hexameric NTPases from dsRNA bacteriophages. Acta Crystallographica Section D: Biological Crystallography, 2003, 59, 2337-2341.	2.5	4
357	Phosphate-recognition sites in catalysis and control of glycogen phosphorylase <i>b</i> . Biochemical Society Transactions, 1987, 15, 1001-1005.	3.4	3
358	Structure of Foot-and-Mouth Disease Virus. , 1990, , 161-171.		3
359	Crystallization and preliminary X-ray analysis of mouse RANK and its complex with RANKL. Acta Crystallographica Section F: Structural Biology Communications, 2009, 65, 597-600.	0.7	3
360	Recording information on protein complexes in an information management system. Journal of Structural Biology, 2011, 175, 224-229.	2.8	3

1

#	Article	IF	CITATIONS
361	Building the atomic model of a boreal lake virus of unknown fold in a 3.9 à cryo-EM map. Journal of Structural Biology, 2018, 202, 94-99.	2.8	3
362	Generation and characterisation of recombinant FMDV antibodies: Applications for advancing diagnostic and laboratory assays. PLoS ONE, 2018, 13, e0201853.	2.5	3
363	Symmetrical arrangement of positively charged residues around the 5-fold axes of SAT type foot-and-mouth disease virus enhances cell culture of field viruses. PLoS Pathogens, 2020, 16, e1008828.	4.7	3
364	Combined Approaches to Study Virus Structures. Sub-Cellular Biochemistry, 2013, 68, 203-246.	2.4	3
365	European Structural Proteomics — A Perspective. , 2008, , 463-504.		3
366	Bacteriophage PRD1 as a nanoscaffold for drug loading. Nanoscale, 2021, 13, 19875-19883.	5.6	3
367	Virus Crystallography. , 1996, 56, 319-364.		2
368	"4D Biology for health and disease―workshop report. New Biotechnology, 2011, 28, 291-293.	4.4	2
369	Universal detection of foot and mouth disease virus based on the conserved VPO protein. Wellcome Open Research, 0, 3, 88.	1.8	2
370	Looking-glass land. Nature, 1989, 338, 196-196.	27.8	1
371	Crystals of the neurotrophins. Protein Science, 1996, 5, 973-977.	7.6	1
372	Crystallization and preliminary diffraction studies of the extracellular region of human p58 killer cell inhibitory receptor (KIR2). Acta Crystallographica Section D: Biological Crystallography, 1998, 54, 433-435.	2.5	1
373	From SPINE to SPINE-2 complexes and beyond. Journal of Structural Biology, 2011, 175, 105.	2.8	1
374	Louise N. Johnson 1940–2012. Nature Structural and Molecular Biology, 2012, 19, 1216-1217.	8.2	1
375	Structure of the regulatory domain of the LysR family regulator NMB2055 (MetR-like protein) from <i>Neisseria meningitidis</i> . Acta Crystallographica Section F: Structural Biology Communications, 2012, 68, 730-737.	0.7	1
376	Ptychographic Single Particle Analysis for Biological Science. Microscopy and Microanalysis, 2021, 27, 190-192.	0.4	1
377	Sample Preparation and Data Collection for High-Speed Fixed-Target Serial Femtosecond Crystallography. Protocol Exchange, 0, , .	0.3	1

378 Virus crystallography. , 2007, , 245-264.

#	Article	IF	CITATIONS
379	Bluetongue virus: the role of synchrotron radiation. Journal of Synchrotron Radiation, 1999, 6, 865-874.	2.4	Ο
380	The crystal structure and dimerization of a co-stimulator B7-1. Seibutsu Butsuri, 2000, 40, S30.	0.1	0
381	Structural studies on the leukocyte co-stimulatory molecule, B7-1. , 2001, , 63-72.		0
382	Molecular recognition by Ig-like receptors, KIRs and Fcl 3 Rs. , 2001, , 45-54.		0
383	High-throughput cloning, expression, and purification. , 2007, , 23-44.		Ο
384	Virion Structure. , 0, , 57-71.		0
385	iNEXT-Discovery and Instruct-ERIC: Integrating High-End Services for Translational Research in Structural Biology. Journal of Visualized Experiments, 2021, , .	0.3	Ο
386	Title is missing!. , 2020, 16, e1008828.		0
387	Title is missing!. , 2020, 16, e1008828.		Ο
388	Title is missing!. , 2020, 16, e1008828.		0
389	Title is missing!. , 2020, 16, e1008828.		Ο
390	Title is missing!. , 2020, 16, e1008828.		0
391	Title is missing!. , 2020, 16, e1008828.		0
392	Purification of African Swine Fever Virus. Methods in Molecular Biology, 2022, 2503, 179-186.	0.9	0